XVIII IMEKO WORLD CONGRESS
Metrology for a Sustainable Development
September, 17 – 22, 2006, Rio de Janeiro, Brazil

INVESTIGATION OF DYMANIC PROPERTIES OF LINE SCALE CALIBRATION SYSTEMS

Saulius Kaušinis [1], *Aurimas Jakštas* [2], *Rimantas Barauskas* [3], *Albinas Kasparaitis* [4]

[1] Department of Mechanical Engineering Kaunas University of Technology, Kaunas, Lithuania, saulius.kausinis@ktu.lt
[2] Department of Mechanical Engineering Kaunas University of Technology, Kaunas, Lithuania, aurimas.jakstas@ktu.lt
[3] Department of System Analysis Kaunas University of Technology, Lithuania, rimantas.barauskas@ktu.lt
[4] Department of Machine Building Vilnius Gediminas Technical University, Lithuania, a.kasparaitis@bsp.lt

Abstract: The paper addresses the error-related problems specific to line scale calibration in dynamic mode of operation that are caused primarily by geometrical and thermal deviations of the calibration system components. A new 3D finite element model has been developed in order to both investigate thermo-mechanical processes in the comparator structure and evaluate possible temperature influence on geometrical dimensions of the line scale. An interferometer-controlled comparator setup with a moving microscope has been designed to evaluate the performance of the long scale calibration process.

Keywords: line scale calibration, FE modelling

1. INTRODUCTION

The need for productivity improvements in line scale calibration ultimately drives demand for technologies, which permit graduation line detection and position measurements in a short time, i.e. calls to introducing dynamic regime of operation.
The major improvements of machine visions systems and new tools such as fast digital cameras, new illumination systems as well as new image scanning and processing technologies and standards allow for high-speed imaging, higher data transfer rates and permit much greater scanning speeds in low light than previously available ones. With faster processors, modern systems can both acquire more information from cameras at faster frame rates and take advantage of more complex line/edge detection algorithms. This makes it possible to build a high-speed image capture and analysis system to meet particular needs of calibration of precision line scale.
Satisfying new demanding and contradictory requirements of high speed and accuracy for precision line scale calibration calls for necessity to investigate properties and dynamics-induced errors of such systems caused by measurement speed fluctuations, time delays, noise and vibrations especially during the graduation line detection.
Mechanical limitations for the calibration systems are featured by the whole complex mechanical system including error compensation circuits. Error-related problems specific to length measurements are caused primarily by geometrical and thermal deviations of the comparator components and the scale.
Nevertheless modern technologies available enable precision line/edge detection in dynamic mode of measurement with a speed up to 20 mm/s. They allow the line scale calibration with measurement uncertainty less than 40 nm/m and ensure the graduation line detection repeatability of 5 nm, [1].
The paper describes the recent joint work performed at Kaunas University of Technology and Brown & Sharpe-Precizika in precision length metrology aimed at the development of an interferential comparator with moving microscope for line scale calibration up to 3.5 m length. The research has been focused on the dynamic mode of calibration and simultaneous evaluation of the influence of dynamic and thermal factors upon the inaccuracies of measurement. A precision interferometer-controlled setup with NIKON modular CCD microscope has been designed in order to carry out the experiments.

2. FEM SIMULATIONS

The state-of-the-art FE technique has been applied in order to evaluate the possible influence of dynamic and thermal factors upon the inaccuracies of measurement. The investigation has been performed by ANSYS finite element software [2].
Heat transfer inside of the structure caused by external temperature field may cause non-homogeneities of the temperature field inside of the structure and leads to undesirable deformations due to the thermal expansion. Effects of such kind in the corps of the comparator have been described in detail [3].
In this work we analyze the elastic displacements of the structure as a response to applied dynamic excitations by employing the linear spectral method and assuming that the acceleration a(t) of the comparator foundation is known, Fig.1. In the scope of precise measurements the main focus is the relative displacement pattern of the measurement zone rather than stresses and strains. In addition, we took into account the elasticity of thread and guide joints between certain parts of the support, which may be influenced by the temperature effects, geometrical inaccuracies and other

factors. The sub-model of the thread joint and guide joint has been investigated in order to evaluate its stiffness.

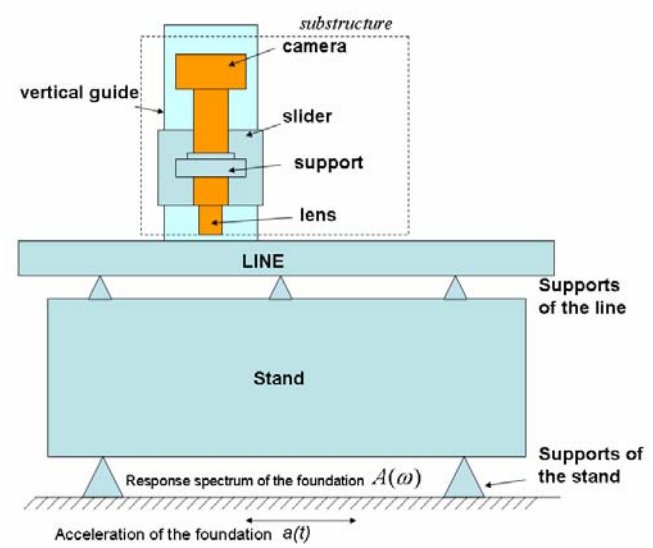

Fig. 1. The scheme of the length comparator with the microscope

2.1. Vibration analysis

In the general 3D case where vibration time law of the foundation is prescribed as the nodal displacement vector $\{U_K(t)\}$, we present the finite element structural equation in the block form as

$$\begin{bmatrix}[M_{NN}] & [M_{NK}]\\ [M_{KN}] & [M_{KK}]\end{bmatrix}\begin{Bmatrix}\{\ddot{U}_N\}\\ \{\ddot{U}_K\}\end{Bmatrix}+\begin{bmatrix}[C_{NN}] & [C_{NK}]\\ [C_{KN}] & [C_{KK}]\end{bmatrix}\begin{Bmatrix}\{\dot{U}_N\}\\ \{\dot{U}_K\}\end{Bmatrix}+ +\begin{bmatrix}[K_{NN}] & [K_{NK}]\\ [K_{KN}] & [N_{KK}]\end{bmatrix}\begin{Bmatrix}\{U_N\}\\ \{U_K\}\end{Bmatrix}=\begin{Bmatrix}\{0\}\\ \{R\}\end{Bmatrix} \quad (1)$$

where nodal displacement vectors $\{U_N(t)\}$, $\{U_K(t)\}$ correspond to unsupported and seismically excited nodes the displacements of which are investigated with respect to immovable reference systems, $[K]$, $[M]$, $[C]$ are stiffness, mass and damping matrices of the structure presented in the block form in accordance with blocks $\{U_N(t)\}$, $\{U_K(t)\}$ of the displacement vector, and $\{R\}$ is nodal reaction force vector of seismically excited nodes. The displacements of unsupported nodes are presented by separating the relative components of the displacements with respect to moving foundation as $\{U_N\}=\{U_{Nrel}\}+\{U_{Nk}\}$. The displacements described by components $\{U_{Nk}\}$, $\{U_K\}$ present the rigid body motion of the structure and do not create internal elastic forces. In the case of proportional damping $[C]=\beta[K]$, after performing the necessary algebraic manipulations the structural equation finally reads as

$$[M_{NN}]\{\ddot{U}_{Nrel}\}+[C_{NN}]\{\dot{U}_{Nrel}\}+[K_{NN}]\{U_{Nrel}\}=[\hat{M}] \quad (2)$$

where $[\hat{M}]=[M_{NN}][K_{NN}]^{-1}[K_{NK}]-[M_{NK}]$.

The left-hand side of equation (2) presents the structural matrices of the structure fixed at nodes of seismic excitation, and the right hand side contains inertia forces acting at each node of the structure in the case of seismic excitation $\{U_K(t)\}$.

In modal coordinates of an undamped structure equation (2) reads as

$$\ddot{z}_i+2\omega_i\vartheta_i\dot{z}_i+\omega_i^2 z_i=\{y_i\}^T[\hat{M}]\{\ddot{U}_K\},\ i=1,2,\ldots,n \quad (3)$$

where $\{U_N\}=\{y_1\}z_1+\{y_2\}z_2+\ldots+\{y_n\}z_n$, $\omega_1,\omega_2,\ldots,\omega_n$ - the natural frequencies of the structure, $[Y]=[\{y_1\},\{y_2\},\ldots,\{y_n\}]$ - the natural forms of the structure, ϑ_i - the damping ratio of the i-th mode.

The nodal acceleration vector on the right hand side of (3) can be generally presented as $\{\ddot{U}_K\}=\{V\}a(t)$, where $\{V\}$ – known vector which is specific for each investigated structure, $a(t)$ – prescribed acceleration time law of the foundation.

In accordance with the linear spectral method, the maximum displacements of each point of the structure are obtained by combining the maximum displacements of each mode. The seismic loading is transformed to the response spectrum of each node of the structure foundation. The value of the displacement response spectrum $D(\omega)$ at frequency ω is obtained as maximum deflection of the linear oscillator loaded seismically by acceleration $a(t)$ as

$$\ddot{x}+2\omega\vartheta\dot{x}+\omega^2 x=a(t) \quad (4)$$

during the time interval of the seismic loading $a(t)$.

Acceleration response spectrum $A(\omega)$ is a relationship of values of maximum acceleration of the linear oscillator (4) seismically subjected to acceleration $a(t)$ against natural frequency ω during the time interval of action of $a(t)$. The displacement and acceleration response spectra are related as $D(\omega)=\dfrac{A(\omega)}{\omega^2}$.

The maximum displacement of the i-th mode is obtained as

$$z_{i\max}=\frac{A(\omega_i)}{\omega_i^2}\{y_i\}^T[\hat{M}]\{V\} \quad (5)$$

which gives maximum displacements of the nodes as

$$\{q_i\}=z_{i\max}\{y_i\} \quad (6)$$

For evaluation of the total of contributions of all modes to the response spectrum, the grouping formula is used as [4]

$$q_j=\sqrt{\sum_{k=1}^{n}\sum_{l=1}^{n}\varepsilon_{kl}\left|q_{jk}\,q_{jl}\right|} \quad (7)$$

where $\varepsilon_{ij} = \begin{cases} 1, & \frac{\omega_k - \omega_{k-1}}{\omega_k} \le 0.1 \\ 0, & \frac{\omega_k - \omega_{k-1}}{\omega_k} \ge 0.1 \end{cases}$, q_j – maximum displacement in j-th d.o.f., n - number of natural frequencies.

If the linear spectral method is to be applied to the substructure of the overall structure, the response spectrum is recalculated from the point of the foundation to the point of attachment of the substructure. The recalculation is performed by investigating a series of finite element models obtained by "scanning" the frequency interval with different values ω. Each model provides a single point to the response spectrum of the point of attachment of the substructure (support) as shown in Fig.2. A sample acceleration response spectrum of the point of attachment of the support is presented in Fig.3 .

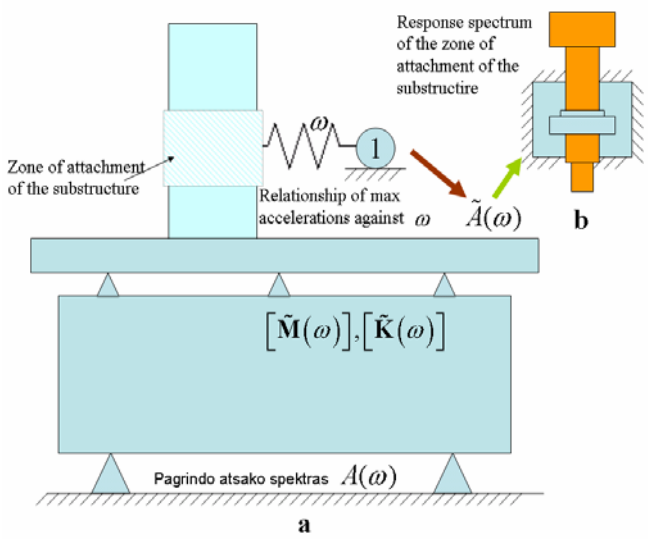

Fig. 2. Recalculation of the response spectrum from the foundation zone to the zone of attachment of the substructure.

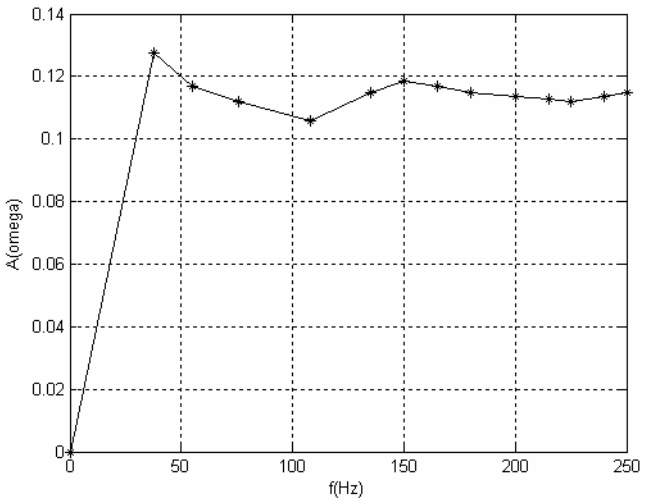

Fig. 3. Sample acceleration response spectrum of the point of attachment of the support

Fig. 4. presents the finite element model of the microscope and the support by using SOLID45 elements in ANSYS.

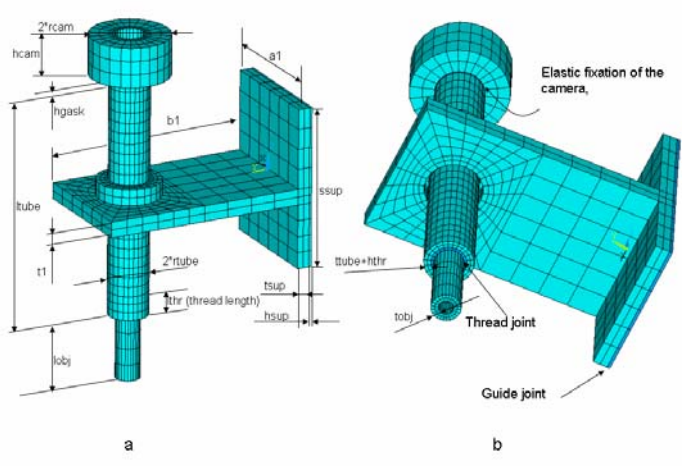

Fig. 4. Finite element model of the microscope and the support

The investigation of very small vibrations of the structure requires the evaluation the flexibility of the thread joint and the guide joint (Fig.4b), which is described by the layer of solid elements of diminished stiffness modulus that relates to the stiffness modulus of the structure as $\frac{E}{E_j} = 1 \div 1000$.

Modal analysis of the substructure fixed at the base of the support has been performed. The analysis of first 9 modes demonstrated that at $\frac{E}{E_j} < 100$ the physical essence of the natural forms remains unchanged and only values of natural frequencies are influenced by additional flexibility at the joint. At $\frac{E}{E_j} > 100$ the natural forms exhibit substantial transformations with respect to the source structure. The relationships of natural frequencies against ratio $\frac{E}{E_j}$ are presented in fig 5.

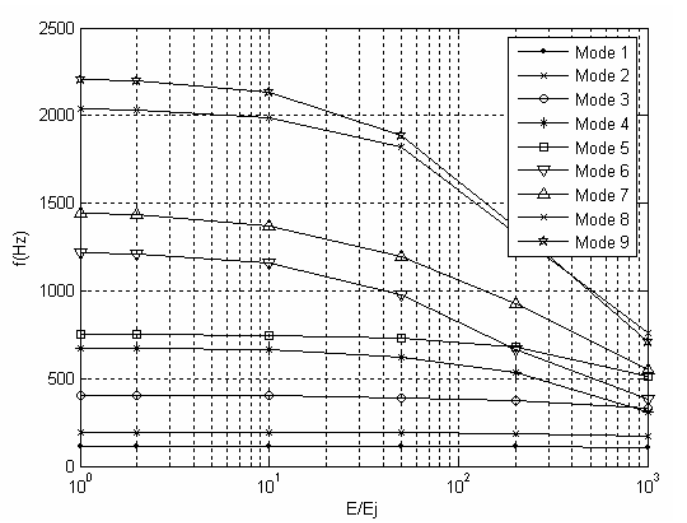

Fig. 5. The relationships of natural frequencies against ratio E/E_j

The contours of maximum displacements of the support with the microscope are presented in Fig.6a . The displacements should be interpreted as maximum values, which the nodes of the structure may assume over the excitation time, however, not necessarily at the same time moments. Maximum displacements are obtained at the front lens of the objective. The displacement of the front lens against the equivalent stiffness of the joints is presented in Fig.6b.

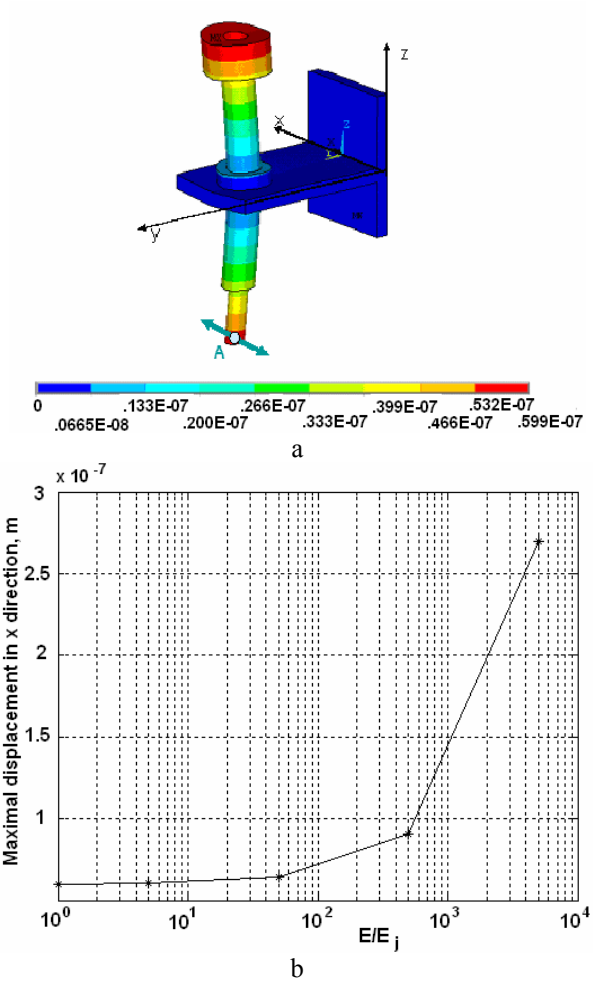

Fig. 6. a - Contours of maximum displacements of the structure during seismic excitation in x direction ; b - the relationship of the max displacement of the front lens against the stiffness of the joint

2.2. Defocusing

For precision quantitative analysis of line profile images high quality digital images are necessary. The accuracy of images captured by photoelectrical microscopes is limited by the accuracy and stability of geometrical dimensions of optical components as well as the capabilities of digital imaging. The specimen must be brought into focus, i.e. the focal plane of the microscope must coincide with the plane of measured line profile before taking an image and measuring any feature. In case the microscope slide is not perfectly perpendicular with respect to the optical axis of the imaging system possible contributions to uncertainty budget from line position sensing may occur due to improper adjustment of measurement line, focus variation (defocusing), microscope axis alignment and other factors.

A common problem in length metrology of line standards is the determination of the exact location of an edge. In practice, however, exact edge information is generally impossible to obtain. Since precision graduated scales have to be calibrated within the range of some parts of a micron it is essential to locate the edge with very high precision through the use of sub-pixeling techniques.

The image of complex structures can be considered as the linear superposition of the image of a single point source. The performance of a microscope is described not only by the magnification and the numerical aperture of the objective. A more complete approach to describe the imaging system is to determine the point spread function (PSF) in spatial domain or optical transfer function (OTF) in frequency domain [5]. If the image of a point source is known, it is possible to predict the image of any object imaged with the system. The image of the point source gives information about the brightness that is transmitted through the optical system, the distortion introduced by the optics, and the maximal possible resolution.

The image acquisition model of the microscope and CCD element is presented as:

$$I(\omega) = \frac{1}{2\pi}\{O(\omega)\cdot OTF(\omega)\cdot B(\omega)\}\otimes S(\omega) \qquad (8)$$

where O, OTF, B, S and I are respectively the intensity of the object in Fourier domain, optical transfer function of the microscope, transfer function of a CCD pixel, sampling function of CCD and image intensity sampled with CCD [5].

The microscope projects the line profile onto CCD element; the back focal plane of the microscope objective lens contains the Fourier transform of the image plane and the finite aperture of the microscope acts as a low-pass filter. The projected image is sampled by the square pixels of the CCD element. The magnification of the microscope is included in the CCD element by reducing the size and spacing between pixels.

The image of the profile is read as discrete output image $i[n,m]$, where n and m are the number of rows and columns of CCD matrix. The efficiency of capturing images generated by an optical microscope onto the pixel array of a CCD depends upon several factors, ranging from the degree of microscope defocusing Δz , objective magnification M and numerical aperture NA to the CCD array size and the dimensions of individual pixels within the array.

When we want to measure any feature of images recorded by camera it is important to know how the original image is sampled by the camera pixels and digitized in order to convert the amplitude of a signal into finite number of discrete levels. The number of pixels in rows and columns and size of individual pixel outline the resolution of the camera.

With reference to equation (7) the simulation of acquisition of the line profile image has been conducted using MATLAB and assuming that the size of CCD camera is 512x512 pixels and pixel size of 6.8x6.8 μm. The intensity profiles from graduation line images have been calculated

varying defocus parameter Δz of the microscope and the midline position of the profile detected.

In general focused images contain higher frequency components than defocused images of a scene. The effect of defocusing on optical image of the line profile creates blurring in the image; it gradually cuts out parts of the object as they move away from the focal plane. The practical consequence is that these parts become darker and eventually disappear. This degraded image is further being processed by CCD camera, which in turn is effected by various noise sources such as photon noise, readout noise, dark current, quantization noise and other factors. Although modern CCD cameras are mainly limited by photon noise, quantization noise that is inherent to the quantization of the pixel amplitudes into a finite number of discrete levels by the analog-to-digital converter also can contribute to the uncertainty of localization of profile edges. Suppression of high frequency components in the image due to defocusing leads to a certain misrepresentation of the amplitude of optical signal.

In the actual measurements the line image is analyzed and the average profile of graduation line is obtained by summing picture element intensities of each row from the area of a window defined by CCD matrix. The middle point of the line profile is obtained by averaging of rising and falling edges from the interval indicated by lower und upper threshold values; typically it ranges from 0.45 to 0.8. This method allows good measurement results if the profile of the line is symmetrical [6].

The results of modeling and calculations performed in order to evaluate both the influence of defocusing of scanning mechanism and angular alignment errors resulting from mechanical deformations of line scale or microscope construction are presented in Fig. 7.

It can be seen that even relatively small angular misalignment increases the error of line centre detection significantly when microscope is out of focus. Therefore the influence of geometrical errors on performance of the measurement system and its nonlinearities can be reduced by a proper arrangement of the scanning system and the line scale.

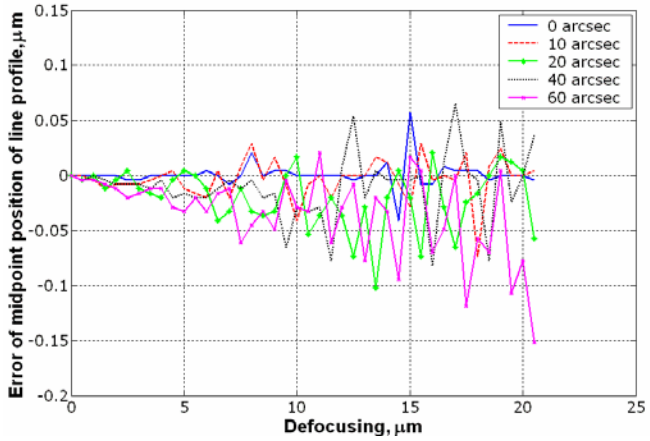

Fig. 7. Error of midline position of line profile vs defocusing of the microscope at various angular deviations between the line scale and microscope

3. EXPERIMENTAL INVESTIGATIONS

In order to examine the calibration process in real time, the experiments of the line scale calibration with a moving CCD microscope have been carried out in specific operating modes, and the accuracy of dynamic calibration has been studied

For precise and full-scale evaluation of the application of dynamic mode of the line scale calibration a CCD-microscope based edge detection system has been developed, [7]. The system uses a modular focusing unit to capture image data and incorporates a set of high-quality objectives and image-processing software. Good quality images of the precision graduation structures have been obtained, and average profiles of the graduation lines have been examined.

A series of measurements have been conducted in order to investigate the calibration capabilities of graduated line scales.

The measured performances confirm that investigated measurement system can operate reliable at velocities up to 15-25 mm/s without appreciable loss in measurement accuracy.

4. CONCLUSION

Error-related problems specific to a precision line scale calibration in dynamic regime were investigated. Advanced FE modelling techniques were applied in order to represent the structural behavior of the comparator. A novel FE model has been developed and influences of dynamic processes in the length comparator structure and possible variations of geometrical dimensions of the line scale and the microscope that lead to increasing measurement uncertainty of line scale measurements has been evaluated. The modelling tools developed enable us to represent the structural behaviour of the calibration system and ensure a high level of adequacy of model to the reality.

Modelling of seismic excitations in the comparator structure has shown that maximum displacements are expected at the bottom plane of the microscope objective and can amount more than 100 nm.

The image acquisition model of optical microscope and CCD camera has been worked out and the influence of microscope defocusing on line detection accuracy has been evaluated. Deviations of the comparator components induced by dynamic processes can significantly decrease the line detection accuracy due to defocusing. These errors can be reduced by proper alignment of the scanning system and the line scale as well as by the use of error compensating algorithms.

The measured performances confirm that investigated measurement system can operate reliable at velocities up to 15-25 mm/s without appreciable loss in measurement accuracy.

REFERENCES

[1] H. Bosse, J. Flügge, "Requirements and recent developments in high precision length metrology" Proceedings of the 159. PTB-Seminar, 2001, pp. 235.

[2] R. Barauskas: Techniques in the Dynamic Analysis of Structures with Unilateral Constraints (Structural Dynamic Systems Computational Techniques and Optimization: Nonlinear Techniques, Gordon and Breach Science Publishers, pp.131-194, 1999.

[3] A. Jakstas, S. Kausinis, R. Barauskas, "Modelling of precision line scale comparator", Mechanika No.2, v.58, pp. 52-57, 2006.

[4] ANSYS Users Manual. Volume 4. Theory. Upd0 DN-R300:50-4-1.

[5] F. R Boddeke, L. J van Vliet, H. Netten,. and I. T Young Autofocusing in microscopy based on the OTF and sampling.-Bioimaging, 1994, No.2, pp.193-203.

[6] A. Lassila, E. Ikonen, K. Riski, "Interferometer for calibration of graduated line scales with a moving CCD camera as a line detector", Applied Optics No.16, v.33, pp. 3600-3603, 1994

[7] A. Jakštas, S. Kaušinis and J. Flügge, "Investigation of calibration facilities of precision line scales", Mechanika, No.3 v.53, pp. 62-67, 2005.